

Unusual Magneto-Optical Phenomenon Reveals Low Energy Spin Dispersion in the Spin-1 Anisotropic Heisenberg Antiferromagnetic Chain System $\text{NiCl}_2 - 4\text{SC}(\text{NH}_2)_2$

S. Cox,¹ R. D. McDonald,¹ M. Armanious,² P. Sengupta,³ and A. Paduan-Filho⁴

¹National High Magnetic Field Laboratory, Los Alamos National Laboratory, MS-E536, Los Alamos, New Mexico 87545, USA

²College of Optical Sciences, University of Arizona, Tucson, Arizona 85721, USA

³Theoretical Division, Los Alamos National Laboratory, Los Alamos, New Mexico 87545, USA

⁴Instituto de Física, Universidade de Sao Paulo, 05315-970 Sao Paulo, Brazil

(Received 23 March 2008; published 21 August 2008)

Electron paramagnetic resonance measurements of $\text{NiCl}_2 - 4\text{SC}(\text{NH}_2)_2$ reveal the low-energy spin dispersion, including a magnetic-field interval in which the two-magnon continuum is within $k_B T$ of the ground state, allowing a continuum of excitations over a range of k states, rather than only the $k = 0$ single-magnon excitations. This produces a novel *Y* shape in the frequency-field EPR spectrum measured at $T \geq 1.5$ K. Since the interchain coupling $J_\perp \ll k_B T$, this shape can be reproduced by a single $S = 1$ antiferromagnetic Heisenberg chain with a strong easy-plane single-ion anisotropy. Importantly, the combination of experiment and modeling we report herein demonstrates a powerful approach to probing spin dispersion in a wide range of interacting magnetic systems without the stringent sample requirements and complications associated with inelastic scattering experiments.

DOI: [10.1103/PhysRevLett.101.087602](https://doi.org/10.1103/PhysRevLett.101.087602)

PACS numbers: 76.30.-v, 75.10.Pq, 75.50.Ee, 78.20.Ls

The essence of correlated spin system physics is understanding the novel properties that arise from interactions between local moments. For extended solids and the energy scales of interest, these are predominantly exchange interactions that give rise to dispersive modes of the spin excitation spectrum. Herein, we demonstrate measurement of this dispersion, and hence the interactions, without the usual complications of inelastic neutron scattering: required sample volume (typically greater than 50 mg, here we can measure 1 mg), expense and availability of beam time, and the possibility of diffuse scattering in hydrogen-rich organic magnets masking the coherent response.

Probing finite momentum states (i.e., dispersion) conventionally requires a transfer of momentum from the probe (particle), and energy and momentum resolution of the scattering event; by contrast, we demonstrate that an optical absorption measurement with negligible momentum transfer and only energy sensitivity can yield similar information. The candidate material for this demonstration is a Ni spin-1 chain that has roused significant scientific interest in its own right.

Spin-1 antiferromagnetic (AFM) chains have prompted considerable interest over recent years, due to the possibility of measuring the gap predicted by Haldane [1–3] or the spin $\frac{1}{2}$ end chain collective excitations that arise in these systems [4]. In addition, since there is always a finite interchain coupling J_\perp , such systems are candidates for the observation of Bose condensation of magnons in gapped quantum magnets [5].

In this Letter, we report the experimental measurement of unusual low-energy magneto-optical excitations in the spin-1 chain compound $\text{NiCl}_2 - 4\text{SC}(\text{NH}_2)_2$ that possess a novel “*Y*”-shaped frequency–field relationship. This observation is the consequence of a field-induced evolution of

the spin excitation spectrum into a state where the two-magnon continuum is accessible at sufficiently low frequency and temperature; we were able to observe this feature because our apparatus is optimized for low frequencies ($f < 65$ GHz), whereas previous studies have focused on high-frequency data ($f > 100$ GHz) [6,7]. The tail of the “*Y*” is caused by contributions from the dispersive magnon continuum, while the upper branches correspond to the finite energy of the top of the single-magnon band; thus, such data show that it is possible to observe effects of the spin dispersion relation in an electron-paramagnetic-resonance (EPR)-type experiment, rather than just the $k = 0$ single-magnon excitations. At temperatures $T \gg J_\perp$, a single $S = 1$ antiferromagnetic Heisenberg chain is able to reproduce the “*Y*”-shaped frequency–field relationship, as well as the width of the magneto-optical features, enabling a quantitative check of the exchange parameters that determine the spin dispersion in $\text{NiCl}_2 - 4\text{SC}(\text{NH}_2)_2$.

Though considerable theoretical effort has been invested in understanding spin-chain systems [8] and related phenomena [9], examples of compounds where these effects can be observed and quantitatively analyzed have been relatively rare [10]. $\text{NiCl}_2 - 4\text{SC}(\text{NH}_2)_2$ [dichloro-*tetrakis* thiourea-nickel(II), known as DTN] is a quasi-one-dimensional $S = 1$ quantum magnet and one of the rare examples of a candidate compound for a field-induced Bose Einstein condensate (BEC) of magnons [11,12]. DTN possesses a strong easy-plane anisotropy D and a paramagnetic ground state which is separated from the first excited state by a finite gap [12]. This organic compound is unique in that it is the only BEC candidate containing Ni ($S = 1$) (most of the other systems contain $S = \frac{1}{2}$ Cu dimers with a singlet-triplet gap determined by the intra-

dimer exchange). In an axially symmetric spin-1 system, there are two possible types of single-ion anisotropy: easy-axis ($D < 0$) and easy-plane ($D > 0$), where D sets the energy scale of the anisotropy term, DS_z^2 . To allow for a field-induced BEC, it is necessary to have a strong easy-axis anisotropy $D \gg J$, where J is the dominant (intra-chain) exchange interaction. This property forces the system to be disordered (paramagnetic) at zero field (each Ni ion is predominantly in the $S^z = 0$ state).

DTN was initially identified as host for a BEC quantum phase transition since the field-temperature phase boundary approaches a power law near the quantum critical point, with an exponent $3/2$ that corresponds to the expected value for a three-dimensional system [12]. For this identification to be confirmed, it is necessary to show that the axial symmetry holds and there are no off-diagonal terms in the spin Hamiltonian. High-frequency EPR found no evidence for axial symmetry breaking [6]. The low frequency EPR results presented here also show no evidence of axial symmetry breaking, but they do reveal an unexpected effect as the spin excitation spectrum evolves with field.

Single crystals of DTN of typical size $1 \times 0.5 \times 3 \text{ mm}^3$ were grown by dissolving a large excess of nickel chloride in a saturated aqueous solution of thiourea [13]. The crystals have a tetragonal crystal structure with space group $I4$, and two molecules in the unit cell [11,13]. The parameters in the Hamiltonian have been determined by fitting zero-field inelastic-neutron-scattering data [12], with the accuracy of the model being confirmed by observing high-energy transitions in a related compound [14], and refined using EPR [6]. The anisotropy, interchain, and intrachain exchange parameters for DTN are $D = 8.6 \text{ K}$, $J_{a,b} = 0.18 \text{ K}$, and $J_c = 2.2 \text{ K}$, respectively [6]. EPR spectra of a single-crystal DTN sample were obtained by placing the sample in a cylindrical resonant cavity and measuring the Q -factor of the cavity (proportional to the microwave absorption of the sample [15]) in the frequency range 11–40 GHz using a Hewlett-Packard 8722ET network analyzer. The cavity was placed in a ^4He flow cryostat that was capable of stabilizing temperatures down to $T = 1.5 \text{ K}$; measurements were carried out at 1.5, 5, and 10 K. The external field, applied along the tetragonal c axis, was provided by a 15 T superconducting magnet. Data at higher frequencies around $f \approx 60 \text{ GHz}$ were recorded using a millimeter wave vector network analyzer manufactured by ABmm [16] and a confocal etalon resonator. Sample spectra showing the observed absorption features are shown in Fig. 1.

The ground state of DTN is a quantum paramagnet at low fields due to the strong easy-plane uniaxial anisotropy, D , that forces the spins to be predominantly in the $S_i^z = 0$ state, precluding any magnetic ordering in zero field. With an applied field parallel to the tetragonal c -axis, the energy of the $S^z = -1$ state is lowered due to the Zeeman effect until it becomes degenerate with the $S^z = 0$ state at a

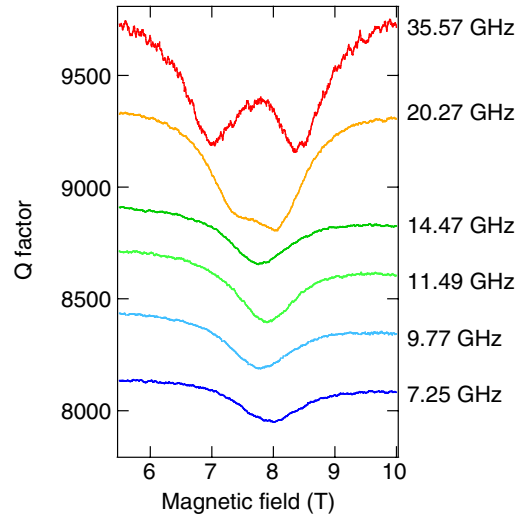


FIG. 1 (color online). Plot of variation of Q factor with magnetic field at various frequencies at 1.5 K, showing how the two peaks present at around 35 GHz gradually coalesce into one peak as the frequency is lowered.

critical field $H_{c1} = 2.1 \text{ T}$ [6]. For $H > H_{c1}$, the mean value of each magnetic moment has a uniform z -component along the field and a staggered xy -component perpendicular to the field (canted antiferromagnet). With increasing field, this canted phase evolves continuously to a fully polarized spin state at $H_{c2} = 12.6 \text{ T}$ [11,12]. In this field range, the multimagnon continuum ($S_z > 1$) is populated such that excitations obeying the optical selection rules ($\Delta k = 0$ and $\Delta S = \pm 1$) can occur for a range of k -states (see Fig. 2). As a result, the frequency-field dependence of the EPR lines contain contributions characteristic of the

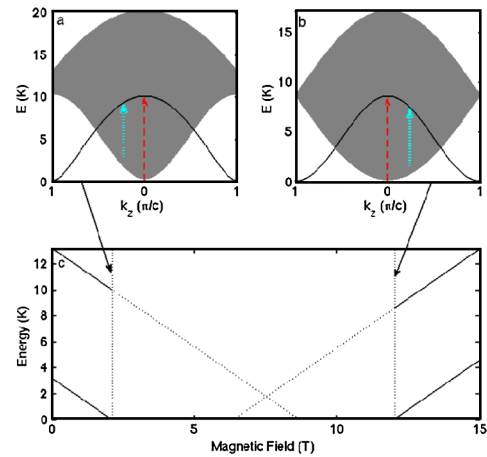


FIG. 2 (color online). The spin dispersion scheme (in arbitrary units) for an $S = 1$ antiferromagnetic chain in the (a) low-field ($B < B_{c1}$) and (b) high-field ($B > B_{c2}$) regimes. The solid line indicates the single-magnon state while the gray shaded area indicates the two-magnon continuum. In both cases, the bandstructure is illustrated at a magnetic field such that the two-magnon continuum is about to touch down, creating a continuum of accessible k -state excitations, as indicated in panel (c).

magnon dispersion. An estimate for the magnitude of the exchange interaction can be extracted from the bandwidth of the dispersion.

The EPR spectrum of this sample clearly shows a single peak which splits into two peaks at high frequencies (see Fig. 1). This gives rise to a “Y” shape when the field at which the resonance occurs is plotted against frequency (see Fig. 3). This differs from the frequency–magnetic-field relationship for an EPR transition between two states that are driven towards degeneracy with magnetic field, which has a characteristic V shape. However, if the two states mix such that they anticross, avoiding degeneracy, the frequency–magnetic-field dependence of the EPR spectral weight remains at finite frequency for all values of magnetic field. The presence of such a U -shaped frequency–field relation, offset to finite frequency, is often taken as a definitive sign of mixing terms in the Hamiltonian (for example off-diagonal exchange terms such as a DM interaction). The novel feature of the Y -shaped frequency–field relationship we observe is that although the upper branches of the Y remain at finite frequency, the spectral weight at lower frequencies (the base of the Y) distinguish this from the anticrossing of energy levels in a nondispersive system. The details of the Y -shape are hence a definitive feature of the dispersion arising from the exchange interactions.

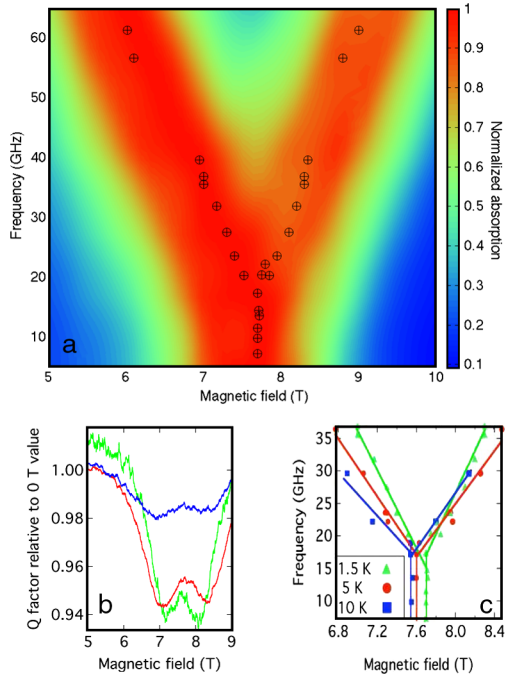


FIG. 3 (color online). (a) Data points: frequency dependence of the peak in absorption as a function of magnetic field applied parallel to the c -axis of $\text{NiCl}_2 - \text{SC}(\text{NH}_2)_2$ at a temperature of 1.5 K. Colored surface: normalized EPR absorption calculated from exact diagonalization of an 8 spin cluster. (b) Shows how the relative size of the Q -factor change at 29 GHz varies with temperature, and (c) shows the variation of the frequency–field relationship with temperature. The lines are a guide to the eye.

At the experimental temperatures ($T \geq 1.5$ K), the interchain interactions are suppressed by thermal fluctuations ($T \gg J_{a,b}$). Hence, a single $S = 1$ antiferromagnetic Heisenberg chain with a strong easy-plane single-ion anisotropy is sufficient to capture the properties of DTN adequately at these temperatures. Consequently, we use the one-dimensional Hamiltonian

$$\mathcal{H} = J \sum_i \mathbf{S}_i \cdot \mathbf{S}_{i+1} + D \sum_i (\mathbf{S}_i^z)^2 - g \mu_B B \sum_i \mathbf{S}_i^z \quad (1)$$

to compute the EPR spectrum, where $J = J_c = 2.2$ K, $D = 8.6$ K, and we ignore interchain coupling ($J_{a,b} = 0$) [10].

At small magnetic fields ($B < B_{c1}$), the ground state of the system is in the quantum paramagnetic phase with $S_z = 0$. The excitation spectrum is gapped, and (at low temperatures) the EPR spectrum consists primarily of the $k = 0$ transition from the ground state to the $S_z = \pm 1$ states with the single-magnon dispersion [shown schematically in Fig. 2(a)]:

$$\epsilon(k, B) = [D^2 + 4DJ \cos(kz)]^{1/2} - g \mu_B B$$

with frequency $\omega = \Delta \pm g \mu_B B$, where $\Delta \approx D + 2J$ (for $D \gg J$) is the energy gap at $k = 0$ and $B = 0$.

At high magnetic fields ($B > B_{c2}$), the ground state of the system is fully spin-polarized. The low-lying excitations consist of a single spin flip from $S_z = 1$ to $S_z = 0$ state that propagates freely through the lattice with momentum \mathbf{k} and kinetic energy proportional to J , the transverse component of the Heisenberg interaction. In this high-field region, the dispersion of the single-magnon excitation is given by the exact expression [shown schematically in Fig. 2(b)]:

$$\epsilon(k, B) = g \mu_B B - D - 2J[1 - \cos(kz)].$$

Since there is no transferred momentum in an EPR transition [Fig. 2(b)], the corresponding frequency is $\omega = \epsilon(k = 0, B) = g \mu_B B - D$, which is identical to that of a single $S = 1$ spin in a magnetic field.

For intermediate fields ($B_{c1} < B < B_{c2}$), the resonant field as a function of frequency smoothly interpolates between the two limits. Note that a measurement of dispersion arising from the exchange interaction is not contingent upon being in the area of the phase diagram that exhibits long range order ($T < 1.2$ K and $2.1 < B < 12.6$ T).

Using these qualitative arguments, we can consider the question of why we see a continuum type spectrum when the high-energy EPR measurements exhibit transitions between discrete levels [6]. We can plot the approximations of the single-magnon dispersion relation given above in the low- and high-field limits (see Fig. 2).

At low temperatures and for low magnetic fields ($B < 2.1$ T), optical transitions (those obeying $\Delta k = 0$ and $\Delta S_z = \pm 1$) will only occur at the zone center. A new situation arises once the single-magnon state (and hence the two-magnon continuum) is within $k_B T$ of the ground

state. Then, optical transitions (again obeying $\delta k = 0$ and $\delta S_z = \pm 1$), will primarily occur for states with a range of absolute k (not just at the zone center) and for a range of energies up to $2J$. This corresponds to the continuous overlap between the $S_z = 1$ and $S_z = 2$ states. The complete EPR signal will also include contributions from transitions between higher excited states.

While the above argument explains the qualitative features of the EPR spectrum, one needs a more rigorous analysis to make quantitative comparisons with the experimental data to validate the model. In a typical EPR experiment, a uniform magnetic field B is applied along the z direction and the measured response to an oscillating magnetic field along the x direction (Faraday configuration) is studied. According to linear response theory, the absorption intensity per unit volume $I(\omega)$ is

$$I(\omega) = \frac{B_R^2 \omega}{2} \chi''_{xx}(q=0, \omega) \quad (2)$$

where B_R is the amplitude of the field along the x direction, and $\chi''_{xx}(q, \omega)$ is the imaginary part of the dynamical susceptibility given by the Kubo formula

$$\chi''_{xx}(q, \omega) = (1 - e^{-\beta\omega}) \times \text{Im} \lim_{\eta \rightarrow 0^+} \int_0^\infty dt e^{-i(\omega - i\eta)t} \langle S_{-q}^\mu(t) S_q^\mu(0) \rangle \quad (3)$$

where $\beta = 1/k_B T$ is the inverse temperature, and S_q^μ is the total spin operator in the momentum space, $S_q^\mu = \frac{1}{\sqrt{N}} \times \sum_{j=1}^N e^{iqj} S_j^\mu$. We used complete diagonalization of H on an $N = 12$ chain to obtain the full eigenspectrum and evaluate Eq. (3).

Figure 3(a) illustrates the superb agreement between EPR data and theoretical simulations. The center of the experimental resonances is marked with black dots; however, as can be seen from Fig. 1, the broadness of the experimental peaks is also a good match to the broadness of the theoretical peaks. These broad peaks in both experimental and theoretical data arise from the numerous overlapping transitions that occur when there is a continuum of k -state excitations. No adjustment of the parameters was needed, indicating that previous refinements [6] have achieved accurate values. It can be seen that the resonances have a full width at half maximum of around 1 T (see Fig. 1), which agrees with the calculated value of around 2 T within the limits of the calculation accuracy imposed by the false structure from finite size effects.

As can be seen from Figs. 3(b) and 3(c), there is no significant change in the shape of the frequency–field relationship up to 10 K. This is as expected since a change should only be observed when the temperature is greater than $D + 2J$ (13 K). The change in the Q factor at resonant absorption relative to the starting Q factor decreases with increasing temperature (see Fig. 3(b)). Above 10 K, no resonance is observed at frequencies below 40 GHz.

In conclusion, we have observed a novel frequency–field relationship in the EPR spectrum of DTN. We have verified

that this feature arises due to the two-magnon continuum touching down, allowing magneto-optical transitions to occur for a range of absolute k . We were able to fit the positions of the observed resonances to a model of the magneto-optical response of weakly coupled $S = 1$ Heisenberg antiferromagnetic (AFM) chains with easy-plane single-ion anisotropy. Similar EPR features to those observed here may also occur in other $S = 1$ antiferromagnetic chain systems such as $\text{Ni}(\text{C}_2\text{H}_8\text{N}_2)_2\text{NO}_2\text{ClO}_4$ [17] and $\text{Ni}(\text{C}_2\text{H}_8\text{N}_2)_2\text{Ni}(\text{CN})_4$ [7]. It is expected that finite momentum transitions between multimagnon states in all correlated systems contribute to the EPR spectral response to a greater or lesser extent depending upon the frequency, temperature, and magnetic-field energies relative to the energy scale of the exchange interactions. The effect may be as simple as linewidth broadening, for which modeling the temperature, frequency, and magnetic-field dependence will yield the exchange energies, or give rise to new and novel frequency–field relationships for the spectra such as the “Y-shape” reported herein.

We thank C. D. Batista, M. Jaime, V. Zapf, and S. Hill for helpful comments. S. Cox acknowledges support from the Seaborg Institute. This research was funded by the U.S. Department of Energy (DoE) under Grant No. LDRD-DR 20070013. Work at NHMFL is performed under the auspices of the NSF, the State of Florida, and the US DoE.

-
- [1] F. D. M. Haldane, Phys. Lett. A **93**, 464 (1983).
 - [2] F. D. M. Haldane, Phys. Rev. Lett. **50**, 1153 (1983).
 - [3] I. Affleck, T. Kennedy, E. H. Lieb, and H. Tasaki, Phys. Rev. Lett. **59**, 799 (1987).
 - [4] E. Polizzi, F. Mila, and E. S. Sorensen, Phys. Rev. B **58**, 2407 (1998).
 - [5] T. Nikuni, M. Oshikawa, A. Oosawa, and H. Tanaka, Phys. Rev. Lett. **84**, 5868 (2000).
 - [6] S. A. Zvyagin *et al.*, Phys. Rev. Lett. **98**, 047205 (2007).
 - [7] S. A. Zvyagin, T. Rieth, M. Sieling, S. Schmidt, and B. Lüthi, Czech. J. Phys. **46**, 1937 (1996).
 - [8] M. Mikeska and M. Steiner, Adv. Phys. **40**, 191 (1991).
 - [9] R. Lai, S. A. Kiselev, and A. J. Sievers, Phys. Rev. B **54**, R12665 (1996).
 - [10] N. Papanicolaou, A. Orendáčová, and M. Orendáč, Phys. Rev. B **56**, 8786 (1997).
 - [11] A. Paduan-Filho, X. Gratens, and N. F. Oliveira, Jr., Phys. Rev. B **69**, 020405 (2004).
 - [12] V. S. Zapf *et al.*, Phys. Rev. Lett. **96**, 077204 (2006).
 - [13] A. Paduan-Filho *et al.*, J. Chem. Phys. **74**, 4103 (1981).
 - [14] M. Orendáč *et al.*, Phys. Rev. B **60**, 4170 (1999).
 - [15] A. Abragam and B. Bleaney, *Electron Paramagnetic Resonance of Transition Ions* (Oxford University Press, New York, 1970).
 - [16] R. D. McDonald *et al.*, Rev. Sci. Instrum. **77**, 084702 (2006).
 - [17] P. P. Mitra and B. I. Halperin, Phys. Rev. Lett. **72**, 912 (1994).